DESIGN, SYNTHESIS AND BIOLOGICAL EVALUATION OF NEW OPIOID ANALGESICS BASED ON TETRAHYDRO-β-CARBOLINE SCAFFOLD IN ZEBRAFISH (DANIO RERIO) LARVAE

WALEED ABDULLAH AHMAD ALANANZEH

UNIVERSITI SAINS MALAYSIA

DESIGN, SYNTHESIS AND BIOLOGICAL EVALUATION OF NEW OPIOID ANALGESICS BASED ON TETRAHYDRO-β-CARBOLINE SCAFFOLD IN ZEBRAFISH (DANIO RERIO) LARVAE

by

WALEED ABDULLAH AHMAD ALANANZEH

Thesis submitted in fulfilment of the requirements for the degree of Doctor of Philosophy

March 2024

ACKNOWLEDGEMENT

First and foremost, praises and thanks go to Allah (SWT), the Most Gracious and the Most Merciful, for His showers of blessings throughout my research work to complete the PhD successfully.

I want to express my deep and sincere gratitude to my supervisor, Prof Dr Mohd Nizam Mordi, Centre for Drug Research (CDR), Universiti Sains Malaysia, for his supervision and invaluable guidance throughout this research project and continuous encouragement during my work.

I want to thank the Center of Drug Research for utilising the facilities to pursue my research. Also, thanks to all Centre for Drug Research technicians and staff, especially Mr Mohd Hilman Sulaiman, Mr Zamri Mohd Zaki, and Mr Mohammad Razak, for their indispensable help and assistance during my research. I want to thank my lab mates, Yusuf Ayipo, Najib Sani, and Saifuldin Arshad, for their stimulating discussions and helpful cooperation.

I proudly thank my late mother and father for their endless love, prayers, and support. I am extremely thankful to my beloved wife for her constant care and support, and to my children, who stood by my side during my journey to finish this work. Also, I thank my sisters and brothers, as well as my father and mother-in-law, for their support and valuable prayers.

Finally, my thanks go to all the people who have supported me in completing the research work directly or indirectly.

TABLE OF CONTENTS

ACK	NOWLE	DGEMENT	ii
TAB	LE OF C	ONTENTS	iii
LIST	OF TAB	LES	vii
LIST	OF FIGU	URES	ix
LIST	T OF SCH	EMES	xvi
LIST	Γ OF SYM	IBOLS	xvii
LIST	T OF ABB	REVIATIONS	xviii
LIST	OF APP	ENDICIES	xxii
ABS	TRAK		xxiii
ABS	TRACT		xxv
CHA	PTER 1	INTRODUCTION	1
1.1	Backgro	ound	1
1.2	Objectiv	/es	9
CHA	PTER 2	LITERATURE REVIEW	10
2.1	Pain		10
	2.1.1	Definition of pain	10
	2.1.2	Classification of pain	10
		2.1.2(a) Pain classification based on duration	10
		2.1.2(b) Pain classification based on tissue damage	11
	2.1.3	Mechanism of pain	12
2.2	G Protei	in-Coupled Receptors (GPCRs) Structure and Function	13
2.3	Mu Opio	oid Receptor (MOR)	15
2.4	Structur	e-Based Drug Design (SBDD)	17
	2.4.1	Structure-Based Drug Design Workflow	18
	2.4.2	SBDD and opioid receptors ligands	19

2.5	Tetrahyd	lro-beta-carbolines (THβC`s)21		
	2.5.1	Tetrahydro-beta-carbolines (THβC`s) occurrence		
	2.5.2	Tetrahydro-beta-carbolines (THβC's) methods of synthesis 22		
	2.5.3	Tetrahydro-beta-carbolines (THβC's) biological activity		
	2.5.4	Tetrahydro-beta-carbolines (THβC`s) in pain management studies		
2.6	The Zeb	rafish (<i>Danio rerio</i>)		
	2.6.1	Zebrafish as a model of <i>in vivo</i> toxicity		
	2.6.2	Zebrafish as a pain model		
CHA	PTER 3	METHODOLOGY		
3.1	Research	n flowchart		
3.2	Compute	ers specifications and software used		
3.3	Molecular modelling			
	3.3.1	Receptor preparation and grid box generation		
	3.3.2	Ligands preparation		
		3.3.2(a) Active MOR ligands		
		3.3.2(b) Tetahydro-beta-carboline analogues		
		3.3.2(c) 6-Methoxytetrahydro-beta-carboline analogues43		
	3.3.3	Molecular docking		
	3.3.4	Physicochemical properties, drug-likeness, pharmacokinetics and toxicity predictions		
	3.3.5	Molecular dynamics simulation and MM-GBSA calculations 45		
3.4	Synthesi	s and characterisation of compounds		
	3.4.1	Materials and chemicals		
	3.4.2	Experimental methods		
		3.4.2(a) Chromatographic techniques		
		3.4.2(b) Products characterisation techniques		
	3.4.3	Selected compounds for synthesis		

		3.4.3(a)	Synthesis of tetrahydro beta-carboline and 6-methoxy tetrahydro beta-carboline by Pictet-Spengler Mechanism	52
		3.4.3(b)	Synthesis N-substituted THβC <i>via</i> alkylation reaction	53
		3.4.3(c)	Dimethylformamide (DMF) solvated alkylation reaction	55
3.5	Biologic	al evaluati	ons	56
	3.5.1	Chemica	ls	56
	3.5.2	Zebrafish	housing and husbandry	57
	3.5.3	Sample p	preparation and chemical exposure	58
	3.5.4	In vivo c	ytotoxicity screening; Fish Embryo Toxicity (FET)	59
	3.5.5	Behaviou	nral study	60
		3.5.5(a)	Pilot study	61
		3.5.5(b)	Analgesic activity study	62
3.6	Statistica	al analysis		64
СНА	PTER 4	RESULT	TS AND DISCUSSION	65
4.1	Molecul	ar modellin	ng	65
	4.1.1	Receptor	s preparation and grid generation	65
	4.1.2	Molecula	nr docking	67
		4.1.2(a)	Validation of docking protocol	68
		4.1.2(b)	Docking of ligands with known activity	70
		4.1.2(c)	Docking of ligands with THβC scaffold	72
		4.1.2(d)	Docking of ligands with 6MTHβC scaffold	81
	4.1.3	Physicoc	hemical and ADMET properties analysis	85
		4.1.3(a)	Analysis of physicochemical properties and drug- likeness	85
			TROTIOSS	
		4.1.3(b)	Pharmacokinetics properties prediction	88

LIST	OF PURI	LICATIO	NC	
APPE	ENDICIES	S		
REFE	ERENCES	S		. 195
5.2	Limitatio	ons and rec	ommendations	. 193
5.1	Conclusi	on		. 191
CHAI	PTER 5	CONCL	USION AND FUTURE RECOMMENDATIONS	. 191
4.4	-		olecular dynamics simulation and MM/GBSA calcul	
4.4	4.3.2		c activity study	
		, ,	Morphological changes	
		. ,	Heart rate	
		, ,	Survival rate	
	4.3.1	Zebrafish	Embryo Toxicity Test (zFET)	. 160
4.3	Biologic	al evaluatio	ons	. 160
		4.2.4(c)	Characterisation results and structural elucidation of other synthesised THβC and THβC analogues	. 137
		4.2.4(b)	Structural characterisation of a representative compound W26	. 131
		4.2.4(a)	Structural characterisation of a representative TH _β C compound W11	. 124
	4.2.4	Synthesis	and characterisation of THβCs	. 122
	4.2.3	Optimisa	tion of the synthesis of N-substituted THβCs	. 121
	4.2.2	Synthesis	s of N-substituted THβCs	. 120
	4.2.1	Synthesis	s of THβC analogues	. 119
4.2	General	procedures	for the synthesis of N-substituted THβCs	. 119
		4.1.4(c)	Binding free energy calculations	.116
		4.1.4(b)	Analysis of ligand-protein interactions	. 108
		4.1.4(a)	Analysis of structural stability and mode of binding	. 100

LIST OF TABLES

	Page
Table 2.1	Proving the generality of the intramolecular allylic alkylation for the synthesis of 4-vinyl-TH β Cs (Bandini et al., 2006)24
Table 2.2	Chemical structures and biological activities of some reported TH β C compounds
Table 3.1	List of solvents, chemicals and materials used in synthesis and structural characterisation
Table 4.1	Docking glide Gscores of known agonists MOR and its residual interaction count against active MOR, PDB ID 6DDE70
Table 4.2	Docking Gscores of the retrieved structures and the original Br fragment obtained from the ZINC database74
Table 4.3	Residual interactions within the binding site of MOR (PDB ID: 6DDE), results were obtained from LIDs of the protein-ligand complexes
Table 4.4	Physicochemical properties and drug-likeness of the designed compounds and two drug controls (SwissAdme)
Table 4.5	Absorption, distribution, metabolism, and excretion properties of the designed compounds and two drug controls92
Table 4.6	Organ toxicity and toxicological endpoint predictions using the ProTox-II web server
Table 4.7	MM-GBSA calculations for selected hit compounds from the last 10 ns of the MD simulation trajectory
Table 4.8	Alkylation reaction optimisation
Table 4.9	Synthesis outcomes of N-substituted THBC derivatives123
Table 4.10	Summarised characteristics of biological evaluations of tested compounds along with their molecular interactions from docking results

Table 4.11	MM-GBSA calculations for selected hit compounds from the	
	whole 100ns of the MD simulation trajectory19	0

LIST OF FIGURES

	Page
Figure 1.1	Intracellular pathways that follow agonist binding to opioid receptors adapted from Azzam et al., 2019
Figure 1.2	Chemical structures of MOR-biased agonists from natural resources.
Figure 1.3	Structures of mitragynine, and tetrahydro-beta-carbolines7
Figure 2.1	Pain pathways and opioid receptors interfere in pain modulation, adopted from Martyn et al., 2019
Figure 2.2	Structure of a G protein-coupled receptor (GPCR). (a) GPCR snake presentation (adopted from www.gpcrdb.org) showing the main structural features; transmembrane helices (TMs), C-terminal helix 8 (H8), extracellular loops (ECLs), and intracellular loops (ICLs) (b) Tertiary ribbon representation of the GPCR structural features including orthosteric binding site
Figure 2.3	A workflow diagram of the structure-based drug design (SBDD) process. Obtained from Batool et al., 2019
Figure 2.4	General structure of carboline alkaloids with the active sites for substitution. Adopted from Szabo et al., 202121
Figure 2.5	A schematic representation of the embryonic developmental stages of zebrafish. Obtained from Rob et al., 2011
Figure 3.1	Research flowchart of the present study; n represents the number of compounds
Figure 3.2	Chemical structures of some active MOR agonists selected from the literature
Figure 3.3	Chemical structures of some active MOR antagonists selected from the literature
Figure 3.4	THβC analogues selected for biological evaluations

Figure 3.5	Summary of the experimental design for the behavioural study of
	test samples in zebrafish larvae
Figure 4.1	A ribbon model of the mu-opioid receptor (MOR PDB 6DDE) embedded in the membrane bilayer illustrates the locations of the orthosteric and allosteric binding sites. DAMGO is shown in the CPK presentation.
Figure 4.2	Protein-ligand interaction diagram for MOR PDB 6DDE with its co-crystallised ligand
Figure 4.3	Self-docking RMSD poses representation. (A) Superimposition of the best pose of the agonist peptide DAMGO (red) and the original co-crystallised pose of DAMGO (green) in the active site of MOR (PDB ID: 6DDE) (black surface). (B) 2D structure of DAMGO 69
Figure 4.4	Pose view showing binding pocket of MOR (PDB ID:6DDE), (A) compound W3 binding pose, (B) compound W1 binding pose79
Figure 4.5	Ligand interaction diagram showing ligands interactions within the binding site of MOR (PDB ID: 6DDE), a) compound W1 and b) compound W3
Figure 4.6	Superimposed structure of compounds W21 and W22 , where the only difference is the methoxy group in W22 . There was no change in the orientation of both ligands in the active site of MOR
Figure 4.7	Superimposed structure of compound W9 (blue) and W10 (red) in the active site of MOR. THβC moiety flipped in W10 after introducing the methoxy group.
Figure 4.8	Binding pose of morphine in the active site of MOR; (a) the pose with interactions that occur more than 30.0% during 50 ns MD simulations, (b) the binding pose retrieved from the docking study.
	99
Figure 4.9	RMSD plots of studied ligands; RMSD of protein C-alpha atoms (blue) and RMSD of ligand in each system (purple)
Figure 4.10	The protein Cα root mean square fluctuation (RMSF) values, averaged over 50 ns MD simulations of; Apo protein (violet),

	Morphine system (black), Naltrexone system (red), W1 system (green), W2 system (blue), W17 system (yellow) and W18 system(brown)
Figure 4.11	The ligand atoms root mean square fluctuation (RMSF) values, averaged over 50ns MD simulations of; Morphine system (black), Naltrexone system (red), W1 system (green), W2 system (blue), W17 (yellow), and W18 system(brown)
Figure 4.12	Secondary Structure Elements (SSE) illustrations for the studied systems over 50 ns MD simulation. The black arrows represent the main changes in the secondary structure
Figure 4.13	2D interaction diagrams of studied ligands during 50 ns MD simulations, showing the protein ligands interactions that lasted for more than 30% of each simulation
Figure 4.14	Protein-ligand interactions in terms of ligand contacts for the studied ligands during 50ns MD simulations, residues show interaction with more than 40% are considered significant
Figure 4.15	GC-MS chromatogram of compound W11 (A) Retention time at 13.99 min, (B) Mass spectrum and (C) The proposed mass fragmentation pathway
Figure 4.16	FTIR spectrum of compound W11
Figure 4.17	¹⁹ F NMR spectrum of W11 (DMSO, 471 MHz) Figure 4.20127
Figure 4.18	¹ H NMR spectrum of W11 (DMSO, 500 MHz)128
Figure 4.19	¹³ C NMR spectrum of W11 (DMSO, 125 MHz)129
Figure 4.20	DEPT 135 NMR spectrum of compound W11 (125 MHz, DMSO)
	129
Figure 4.21	COSY spectrum of compound W11 (500 MHz, DMSO)130
Figure 4.22	HMBC spectrum of compound W11 (500 MHz, DMSO)130
Figure 4.23	GC-MS chromatogram of compound W26 (a) retention time at
	16.0 min, (b) the mass spectrum of compound W26 131
Figure 4.24	Proposed fragmentation pathway of compound W26.

Figure 4.25	FTIR spectrum of compound W26
Figure 4.26	¹⁹ F NMR spectrum of W26 (DMSO, 471 MHz)134
Figure 4.27	¹ H NMR spectrum of W26 (DMSO, 500 MHz)134
Figure 4.28	¹³ C NMR spectrum of W26 (DMSO, 125 MHz)135
Figure 4.29	2D [¹ H, ¹³ C] HMBC spectrum of compound W26 (500 MHz, DMSO)
Figure 4.30	2D [¹ H, ¹³ C] HSQC spectrum of compound W26 (500 MHz, DMSO)
Figure 4.31	Graphical comparison of zebrafish embryo survival rate (%) in the testing solutions. Data are presented in mean \pm SD (n = 30), where * represents groups with significance (p < 0.005)
Figure 4.32	Graphical comparison of heart rate (bpm) of zebrafish larvae in negative and 1%DMSO control and treatment groups. Data are presented in mean \pm SD (n = 30), where * represents groups with significance (p < 0.005).
Figure 4.33	Morphology of zebrafish embryos exposed to 30 μM studied TH βC analogues, negative, positive, and solvent controls at 96-hpf. The purple arrows indicated morphological malformations164
Figure 4.34	Analgesic effect of fentanyl in larval zebrafish. A) Trajectories of movement of larvae across the well, a) control, b) formalin and c) formalin/fentanyl well. B) Swimming velocity changes as per test solution used C) average velocities of the studied group within the time interval 2-7 mins after administration of testing solutions. Data are presented as mean \pm SD of studied groups (n = 20), where * represents groups with significance (p < 0.005)
Figure 4.35	Analgesic effect of W5 in larval zebrafish. A) mean velocity over time. B) average velocities of the studied group within 2-7 mins after administering testing solutions. Data are presented as mean \pm SD of studied groups (n = 24). *p<0.001, **p<0.005 and ***p<0.05.

Figure 4.36	Analgesic effect of W6 in larval zebrafish. A) mean velocity over
	time increased after exposure to the testing solutions. B) average
	velocities of the studied group within the interval 2-7 mins after
	administering testing solutions. Data are presented as mean \pm SD
	of studied groups (n = 21). *p<0.001 and **p<0.01169
Figure 4.37	Analgesic effect of W9 in larval zebrafish. A) mean velocity over
	time. B) average velocities of the studied group within 2-7 min
	after administration of testing solutions. Data are presented as
	mean \pm SD of studied groups (n = 24). *p < 0.001, **p < 0.005 and
	***p < 0.05. Figure 4.46
Figure 4.38	Analgesic effect of W25 in larval zebrafish. A) mean velocity over
	time. B) average velocities of the studied group within the interval
	2-7 mins after administering testing solutions. Statistical analysis
	was done using one-way ANOVA followed by Tukey HSD post
	hoc test. Data are presented as mean \pm SD of studied groups (n =
	20). *p<0.001, **p<0.005 and ***p<0.05
Figure 4.39	Analgesic effect of W26 in larval zebrafish. A) mean velocity over
_	time. B) average velocities of the studied group within 2-7 min
	after administration of testing solutions. Data are presented as
	mean \pm SD of studied groups (n = 23). *p<0.001, **p<0.005 and
	***p<0.05
Figure 4.40	Analgesic effect of W31 in larval zebrafish. A) mean velocity over
-	time. B) average velocities of the studied group within the time
	interval of 2-7 min after administration of testing solutions. Data
	are presented as mean \pm SD of studied groups (n = 22), where *
	represents groups with significance (p < 0.001)
Figure 4.41	Analgesic effect of W32 in larval zebrafish. A) mean velocity over
-	time. B) average velocities of the studied group within the interval
	2-7 mins after administering testing solutions. Data are presented
	as mean \pm SD of studied groups (n = 24). *p<0.001 and **p<0.05.
	176

Figure 4.42	Analgesic effect of W33 in larval zebrafish. A) mean velocity over time. B) average velocities of the studied group within the time interval of 2-7 min after administration of testing solutions. Data are presented as mean \pm SD of studied groups (n = 22). *p < 0.001 and **p < 0.005
Figure 4.43	Analgesic effect of W35 in larval zebrafish. A) mean velocity over time. B) average velocities of the studied group within 2-7 mins after administration of testing solutions. Data are presented as mean \pm SD of studied groups (n = 26). *p < 0.001 and **p < 0.005.
Figure 4.44	Analgesic effect of W36 in larval zebrafish. A) mean velocity over time. B) average velocities of the studied group within 3-7 min after administration of testing solutions. Data are presented as mean \pm SD of studied groups (n = 24). *p < 0.001 and **p < 0.005.
Figure 4.45	Analgesic effect analysis of the most active compounds in larval zebrafish as a mean of average velocities of the effective concentration of the tested compounds W6 , W25 , W31 , W32 , W26 , and W33 within the time interval of 2-7 mints after administration of testing solutions. Data are presented as mean \pm SD of studied groups. ****p < 0.0001, ***p < 0.001 an **P <0.005
Figure 4.46	Time dependent RMSD plots of free (Apo) 6DDE protein (Blue), W25-6DDE complex (brown), W32-6DDE complex (green), and Fentanyl-6DDE complex (Indigo) obtained from 100 ns MD simulation trajectories.
Figure 4.47	Individual amino acids RMSF plots of Free (Apo) 6DDE protein (Blue), W25-6DDE Complex (green), W32-6DDE Complex (red), and Fentanyl-6DDE complex (Indigo) obtained from 100 ns MD simulation Trajectories
Figure 4.48	Time dependent hydrogen bond analysis of W25 -6DDE complex (brown), W32 -6DDE complex (blue), and Fentanyl-6DDE

complex (green) obtained from 100 ns MD simulation trajectories.

LIST OF SCHEMES

	Page
Scheme 2.1	Synthesis of THIQ 2 and THβC 4 via Pictet-Spengler reaction. Obtained from Cox & Cook, 1995
Scheme 2.2	Bischler-Napieralski reaction/cyclisation reaction scheme. Obtained from Laine et al., 2014
Scheme 2.3	 a) Synthesis of THβCs via Pictet–Spengler vs new metal-catalysed reactions. b) Transition metal catalysts for the synthesis of THβC 15. Obtained from Ascic et al., 2012. 25
Scheme 2.4	STR catalyses the condensation of tryptamine 3 and secologanin 16 to give the THβC (S)-strictosidine26
Scheme 3.1	General scheme of synthesis of target THβC scaffolds52
Scheme 3.2	Synthesis of titled compounds using ACN, under reflux for 3 h54
Scheme 3.3	Synthesis of compounds W31 and W32
Scheme 3.4	Synthesis of titled compounds at 0 °C in DMF56
Scheme 4.1	Mechanism of synthesis of THβC and 6MTβC via acid-catalysed Pictet-Spingler reaction
Scheme 4.2	Substitution reaction of THβC with alkyl bromide to form THβC derivatives

LIST OF SYMBOLS

% Percentage

¹H Proton

¹³C Carbon-13

 α Alpha

Å Angstrom Unit

β Beta

br Broad signal

δ Chemical Shift

J Coupling Constant

°C Degree Celsius

d Doublet

m.p Melting Point

μL Microlitre

μM Micromolar

mg Milligram

mL Milliliter

MLogPo/w Lipophilicity

mol Mole

m Multiple

m/z Mass-to-charge ratio

ppm Parts Per Million

LIST OF ABBREVIATIONS

1D One Dimensional

2D Two Dimensional

3D Three Dimensional

5HT 5-hydroxytryptamine

7TMRs Seven Transmembrane Receptors

ADME Absorption, Distribution, Metabolism and Excretion

ADMET Absorption, Distribution, Metabolism, Excretion and Toxicity

AITC Allyl isothiocyanate

AVMA American Veterinary Medical Association

BBB Blood-Brain Barrier

BOILED-Egg Brain Or IntestinaL EstimateD permeation method

BRET Bioluminescence Resonance Energy Transfer

cAMP Cyclic Adenosine Monophosphate

ACN Acetonitrile

CDR Centre for Drug Research

CHARMM Chemistry at Harvard Macromolecular Mechanics

CL Clearance

CNS Central Nervous System

COSY Correlation spectroscopy

Cryo-EM Cryogenic Electron Microscopy

dd Doublet of Doublets

DEPT Distortionless enhancement by polarisation transfer

DHβCs Dihydro-β-carbolines

DIPEA N,N-Diisopropylethylamine

DMF Dimethylformamide

DMSO Dimethyl Sulfoxide

DMSO-d Deuterated Dimethyl Sulfoxide

dpf Day Post Fertilisation

dt Doublet of Triplets

ECLs Extracellular Loops

EtOA Ethyl acetate

FET Fish Embryo Toxicity

FRET Förster resonance energy transfer

FT-IR Fourier transform infrared spectroscopy

GB/SA Generalised-Born surface area

GC-MS Gas chromatography-mass spectrometry

GPCRs G protein-coupled receptors

HBA Hydrogen bond acceptors

HBD Hydrogen bond donors

H-Bond Hydrogen Bond

hERG human ether-a-go-go related gene

HMBC Heteronuclear multiple-bond coherence

HMQC Heteronuclear multiple quantum coherence

hpf Hour Post Fertilisation

HSQC Heteronuclear single-quantum coherence

HTVS High Throughput Virtual Screening

IASP International Association for the Study of Pain

IC₅₀ Half-Maximal Inhibitory concentration

ICLs Intracellular Loops

K₂CO₃ Potassium carbonate

LCMS Liquid Chromatography Mass Spectrometry

LID Ligand interaction Diagram

LogS Solubility constant

MD Molecular Dynamic

MM Molecular Mechanics

MM-GBSA Molecular Mechanics Generalised Born/Solvent Accessibility

MOE Molecular Operating Environment

MOR Mu Opioid Receptor

MR Molecular Refractivity

MW Molecular Weight

NAMs Negative Allosteric Modulators

NMR Nuclear Magnetic Resonance Spectroscopy

NTX Naltrexone

OECD Organisation for Economic Cooperation and Development

OPLS Optimised Potentials for Liquid Simulations

OR Opioid Receptors

PAMs Positive Allosteric Modulators

PB/SA Poisson-Boltzmann surface area

PMF Potential of Mean Force

POPC 1-Palmitoyl-2-oleoylphosphatidylcholine

QSAR Quantitative Structure-Activity Relationships

RMSD Root Mean Square of Deviations

RMSF Root Mean of Fluctuation

s Singlet

SAR Structure-Activity Relationship

SBDD Structure (Target) Based Drug Design

SD Standard Deviation

SDF Structure-Data File

SMILES Simplified Molecular Input Line Entry System

SP Standard Precision docking

SPC Simple Point-Charge

SSE Secondary Structure Elements

t Triplet

td Triplet of Doublet

TEA Triethylamine

TH β C Tetrahydro- β-carboline

TLC Thin Layer Chromatography

TM Transmembrane

TPSA Topological Polar Surface Area

VD Volume Distribution

XP Extra precision docking

zFET ZebraFish Embryo Toxicity Test

βCs Beta-Carbolines

LIST OF APPENDICIES

APPENDIX A LIGAND INTERACTION DIAGRAMS FOR THβC ANALOGUES WITH MOR (PDB ID: 6DDE)

APPENDIX B LIGAND INTERACTION DIAGRAM FOR THE 6MTHβC ANALOGUES WITH MOR (PDB ID: 6DDE)

APPENDIX C NMR and GC-MS SPECTRA

APPENDIX D CRYSTALLOGRAPHIC DATA

REKABENTUK, SINTESIS DAN PENILAIAN BIOLOGI ANALGESIK OPIOID BARU BERDASARKAN KERANGKA TETRAHIDRO-BCARBOLINA DALAM LARVA IKAN ZEBRA (DANIO RERIO)

ABSTRAK

Pengurusan kesakitan yang berkesan memerlukan pendekatan menyeluruh yang merangkumi gabungan campuran intervensi farmakologi dan bukan farmakologi. Analgesik opioid mengurangkan kesakitan dengan bertindak melalui reseptor opioid Mu (MOR) tetapi dikaitkan dengan kesan sampingan yang tidak diingini. Alkaloid tetrahidro-beta-karbolina (THβC) dilaporkan mempunyai pelbagai aktiviti, termasuk kesan analgesik. Mitraginina, suatu struktur berasaskan THBC terbukti mempunyai kurang kesan samping kerana isyarat intraselularnya cenderung terhadap protein G. Kajian ini bertujuan untuk mereka bentuk, mensintesis, dan menilai aktiviti analgesik terbitan THβC. Pangkalan data sebanyak 25,227 analog THβC disediakan daripada saringan maya pangkalan data ZINC untuk fragmen bromin dan seterusnya fragmen tersebut dihubungkan pada kedudukan N2 kerangka THβC. Dengan bantuan pengedokan molekul terhadap keadaan aktif MOR (PDB ID: 6DDE), 20 analog THβC yang mempunyai Gscores daripada pengedokan XP yang lebih baik daripada morfin telah dipilih. Pengubahsuaian lanjut pada sebatian terpilih dengan memasukkan kumpulan metoksi di kedudukan C6 kerangka THβC menghasilkan satu set lagi 20 sebatian analog bagi 6-metoksi THβC (6MTHβC), kesemuanya diramalkan mempunyai sifat ADMET yang baik. Daripada jumlah 40 sebatian THβC/6MTHβC, 38 terbitan berjaya disintesis dan dielusidasikan strukturnya menggunakan kaedah pencirian GC-MS, FTIR, spektroskopi 1D dan 2D NMR. Penilaian toksisiti in vivo 10 wakil terpilih secara rawak daripada analog yang disintesis menggunakan embrio ikan

Zebra menunjukkan bahawa mereka adalah selamat. Aktiviti analgesik menggunakan pergerakan bebas larva ikan Zebra menunjukkan bahawa pendedahan larva kepada pengaruh rasa sakit, formalina merosakkan pergerakan mereka seperti yang ditunjukkan oleh purata halaju 1.60 mm/s berbanding 0.60 mm/s bagi kawalan. Terutamanya, dua daripada 10 sebatian (W25 dan W32) menunjukkan profil analgesik yang paling berpotensi. Halaju, purata larva berkurangan kepada 0.6 mm/s dan 0.7 mm/s apabila terdedah kepada **W25** pada kepekatan 1 µM dan 6 µM masing-masing. Ini konsisten dengan kesan yang direkodkan (0.6 mm/s) oleh fentanil 3 µM. Begitu juga, W32 menunjukkan halaju purata 0.4 mm/s dan 0.5 mm/s pada kepekatan 1 μM dan 6 µM masing-masing. Kedua sebatian, W25 dan W32 mengikat kepada MOR (PDB ID 6DDE), dengan berinteraksi kepada asid amino penting untuk pengaktifan afiniti ikatan yang kuat semasa simulasi MD 100 ns. Penyiasatan teori yang lebih lanjut menyokong potensi mereka sebagai sebatian analgesik yang bertindak melalui pengaktifan MOR. Kesimpulannya, analog THβC yang direka mewakili titik permulaan yang baik untuk merancang agonis reseptor opioid sebagai analgesik masa hadapan. Kajian ini mendedahkan prinsip-prinsip kimia perubatan dari atas ke bawah dalam mereka bentuk drug.

DESIGN, SYNTHESIS AND BIOLOGICAL EVALUATION OF NEW OPIOID ANALGESICS BASED ON TETRAHYDRO-B-CARBOLINE SCAFFOLD IN ZEBRAFISH (DANIO RERIO) LARVAE

ABSTRACT

Effective pain management requires a comprehensive approach that includes a combination of pharmacological and non-pharmacological interventions. Opioid analgesics reduce the pain acting through the Mu opioid receptors (MORs) but are found to be associated with undesired side effects. Tetrahydro-beta-carboline (THβC) alkaloids are reported to possess various biological activities, including analgesic effects. Mitragynine, a THβC-based structure, has been proven to have reduced side effects, as it was found to bias intracellular signaling towards G proteins. The present study aims to design, synthesise, and evaluate the analgesic activities of THβC derivatives. A database of 25,227 THβC analogues was prepared from structure based virtual screening of the ZINC database for bromine fragments and linking the fragments at the N2 position of the THβC scaffold. By the aid of molecular docking against the active state of MOR (PDB ID: 6DDE), 20 THβC analogues had comparatively better XP docking Gscores than morphine were selected. Further modification of the selected compounds by inserting a methoxy group at position C6 of their THβC scaffold afforded another set of 20 compounds of the 6-methoxy THβC (6MTHβC) analogues, altogether predicted with good ADMET properties. From the total 40 THBC/6MTHBC compounds, 38 derivatives were successfully synthesised and structurally elucidated using GC-MS, FTIR, 1D and 2D NMR spectroscopy characterisation methods. In vivo toxicity evaluation of selected 10 representatives of the synthesised analogues using Zebrafish embryos propelled them as non-toxic. Their

analgesic activities using the locomotion activity of freely behaving larval zebrafish showed that exposure of the larvae to a pain inducer, formalin (pain inducer) increased their movement as indicated by an average velocity of 1.60 mm/s compared to the 0.60 mm/s of the control. Notably, two out of the 10 compounds (W25 and W32) demonstrated promising analysesic profiles. The average velocities of the larvae were reduced to 0.6 mm/s and 0.7 mm/s when exposed to W25 at 1 µM and 6 µM respectively. These are consistent with the recorded effects (0.6 mm/s) of the 3 µM fentanyl. Similarly, W32 showed average velocities of 0.4 mm/s and 0.5 mm/s at concentrations of 1 µM and 6 µM respectively. The two compounds, W25 and W32 conferred stability upon binding to the MOR (PDB ID 6DDE), interacting with essential amino acids for activation with strong binding affinities during a 100 ns MD simulation. The theoretical investigation further supports their potential as promising analgesics that suggestively act *via* MOR activation. In conclusion, the designed THβC analogues represent a good starting point for designing opioid receptor agonists as future analgesics. The study reveals the fundamentals of top-down medicinal chemistry approaches in drug design.

CHAPTER 1 INTRODUCTION

1.1 Background

Pain is an unpleasant feeling resulting from injury, damage or changes in any physiological system requiring medical care for millions worldwide (Pratik et al., 2018). Pain can be classified into two main categories; tissue damage level (i.e. nociceptive, neuropathic and nociplastic pain) and duration of pain (i.e. chronic and acute pain) (Chary, 2020). Many reports globally addressed chronic pain as a significant concern due to its impact on patients' quality of life. For example, the estimated prevalence of chronic pain in developed countries was reported in the range of 11% to 40% in the United States (Dahlhamer et al., 2018), 16% to 41% in Canada (Foley et al., 2021; Schopflocher et al., 2011) and 35.0% to 51.3% in the United Kingdom (Fayaz et al., 2016). However, in developing countries like Malaysia, an age-based study estimated the prevalence of chronic pain in the range of 7.0% to 15.3% (Lem et al., 2021; Mohamed & Hairi, 2014), with the highest prevalence of 15.3% among older people.

The experience of pain is the final step in a complex information-processing network of pain mechanisms processed *via* different stages (i.e. transduction, transmission and perception) involving the spinal cord, spinal gating and the brain (Bridgestock, 2013). Antinociceptive (analgesics) are chemicals that reduce pain sensation through a series of processes that occur mainly in the brain (Woolf, 2010) and through the activation of opioid receptors (ORs) (Stein, 2016).

G protein-coupled receptors (GPCRs) represent the largest superfamily of cell transmembrane (TM) receptors (Rosenbaum et al., 2009). Being a bundle of flexible helices of two sides, the extracellular side of GPCRs can bind with a wide range of extracellular molecules at orthosteric and allosteric sites. In contrast, the intracellular side binds mediators, mainly G proteins and beta-arrestins (Mahmod Al-Qattan & Mordi, 2019). The opioid receptors which are members of the GPCR are expressed and distributed within the central nervous system (Sora et al., 1997), peripheral nervous system (Ozawa et al., 2015), the gastrointestinal tract (Galligan, 2016; Sobczak et al., 2014). The mu, delta and kappa opioid receptor subtypes, which are encoded by *Oprm1*, *Oprd1* and *Oprk1* genes, respectively (Kieffer & Gavériaux-ruff, 2002; Stevens, 2009), have been identified to be closely associated with pain perception (Kaserer et al., 2020), reward (Rodriguez-Arias et al., 2010) and neuroprotection (Chao & Xia, 2010). In addition, opioid receptors were found to be activated endogenously by different types of opioid peptides (i.e., enkephalins, beendorphin and dynorphins) (Akil et al., 1998).

The Mu Opioid Receptor (MOR) mediates the most potent antinociceptive effects, the most powerful analgesic and addictive properties of opiate alkaloids (Darcq & Kieffer, 2018). Hence, the MOR is a primary target in developing new analgesics (Law et al., 2013; Pradhan et al., 2012). Binding of the ligand to MOR may result in the intracellular interaction of the Gi protein or induce interaction with beta-arrestin. Upon MOR activation, intracellular interaction with the Gi protein alleviates pain, while interaction with beta-arrestin induces respiratory depression, as illustrated in Figure 1.1(Azzam et al., 2019).

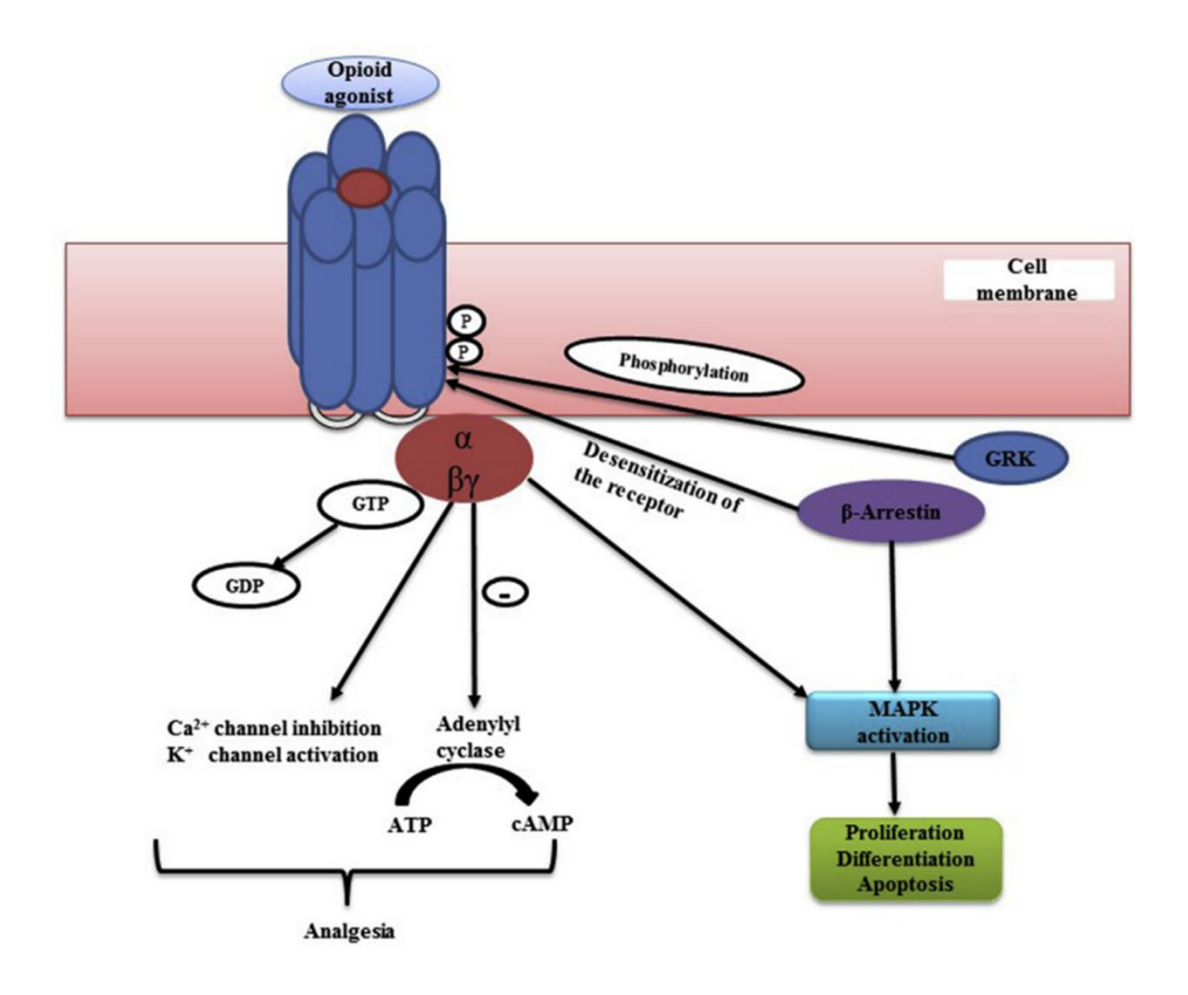


Figure 1.1 Intracellular pathways that follow agonist binding to opioid receptors adapted from Azzam et al., 2019.

Activation of MOR can fall into two opposing pathways: agonist and antagonist. Based on their pharmacological response, agonists fall into two categories: full and partial agonists (Manglik et al., 2015; Nygaard et al., 2013). Full agonists bind to the orthosteric site and stabilise the active conformation of the MOR, leading to a full biological response. While partial agonists bind to the same site but lead to a partial biological response even at higher concentrations (Nygaard et al., 2013). In contrast, antagonists bind to the same orthosteric site without affecting the equilibrium between an active or inactive state and its basal activity. Neutral antagonists block the binding of other ligands without imposing a biological response. Molecules that can suppress basal activity but stabilise the inactive state are called inverse agonists (Manglik et al.,

2015; Nygaard et al., 2013). Signalling through the heterotrimeric G protein Gi results in analgesia, sedation, euphoria, and physical dependence (Chan et al., 2017). MOR can also signal through arrestin, and this pathway has been attributed to the non-desired effects of opioid analgesics (Bohn et al., 2000; Raehal et al., 2005).

Opiates (MOR agonists) are the most common drugs used for treating moderate to severe chronic pain (Trescot et al., 2008). Although they significantly affect pain modulations, they are also associated with several undesired effects, such as respiratory depression, constipation, and nausea. The limitations posed by these undesirable effects restrict the clinical significance of opiates, prompting a quest for opioid drugs that are safer and more suitable for use (Martínez-Navarro et al., 2018). Opioid chemistry has, over time, focused on thebaine-derived alkaloids isolated from poppy (Papaver somniferum). Opioids can be divided into four major classes; (1) endogenous opioid peptides such as dynorphin and met-enkephalin, (2) opium alkaloids such as morphine, (3) semi-synthetic opioids which are derivatives of morphine (4) synthetic derivatives of structures different than morphine such as pethidine, fentanyl, methadone, pentazocine and buprenorphine (Mcdonald & Lambert, 2016; Carlin et al., 2020). Most of the known MOR agonists were discovered through traditional approaches, including; isolation from a natural product such as morphine, by natural product derivatisation such as oxycodone and hydromorphone, or by synthetic manipulation of natural product scaffolds such as fentanyl (Poli et al., 2019). However, as mentioned above, these are potent MOR agonists with addictive abilities and undesired side effects. To overcome the morphine-like side effects, novel approaches are being used, such as biasing the GPCRs over β-arrestin2, designing MOR-positive allosteric modulators (PAMs) (Kandasamy et al., 2021), and designing ligands that possess functional activities such as the NOP/MOR agonists (Ding et al., 2018) and MOR agonists/KOR antagonists (Nastase et al., 2019).

The MOR activation involves several effectors, and biased agonism is considered one of the strategies currently used in drug discovery for safer MOR-targeted therapeutics in pain management with lower side effects (Thompson et al., 2016). Generally, biased agonism, which could refer to ligand functional selectivity upon binding with its receptor, can lead to favouring one signalling pathway over another (i.e., Gi or β -arrestin) (Figure 1.1), which in turn produces either wanted or unwanted effects of the ligand (drug) (Li et al., 2017).

Drug discovery and development efforts have been advanced to discover analysesics that will provide more effective pain relief with selective activation of the Gi/o pathway over the beta-arrestin pathway by biased signalling. These include the designing of analysesics that are deprived of respiratory and addictive side effects. The reported strategies used in designing MOR-biased agonists include:

- (1) Measurement of biased agonism of existing opioid drugs. It has been reported that buprenorphine, despite being a partial agonist against MOR, produces an analgesic effect similar to morphine (Davis et al., 2018). It was the only drug not showing β-arrestin recruitment (Butler, 2013).
- (2) Screening of an internal compound collection of small molecule methods has afforded Oliceridine (TRV130) **2** (Figure 1.2) as a MOR-biased agonist (Chen et al., 2013; Dewire et al., 2013).
- (3) From natural products: The first known biased MOR agonist derived from natural products is Herkinorin 3, obtained as a derivative of salvinorin A 4 (active

substituent from *Salvia divinorum*) (Butelman et al., 2008). Other renowned MOR agonists from natural products include the active constituents of *Mitragyna speciosa*; mitragynine **5**, 7-hydroxy mitragynine **6**, and mitragynine pseudoindoxyl **7**, found to be a biased agonist against MOR (Kruegel et al., 2016; Váradi et al., 2016; Zarembo et al., 1974). The chemical structures of these natural products are displayed in Figure 1.2.

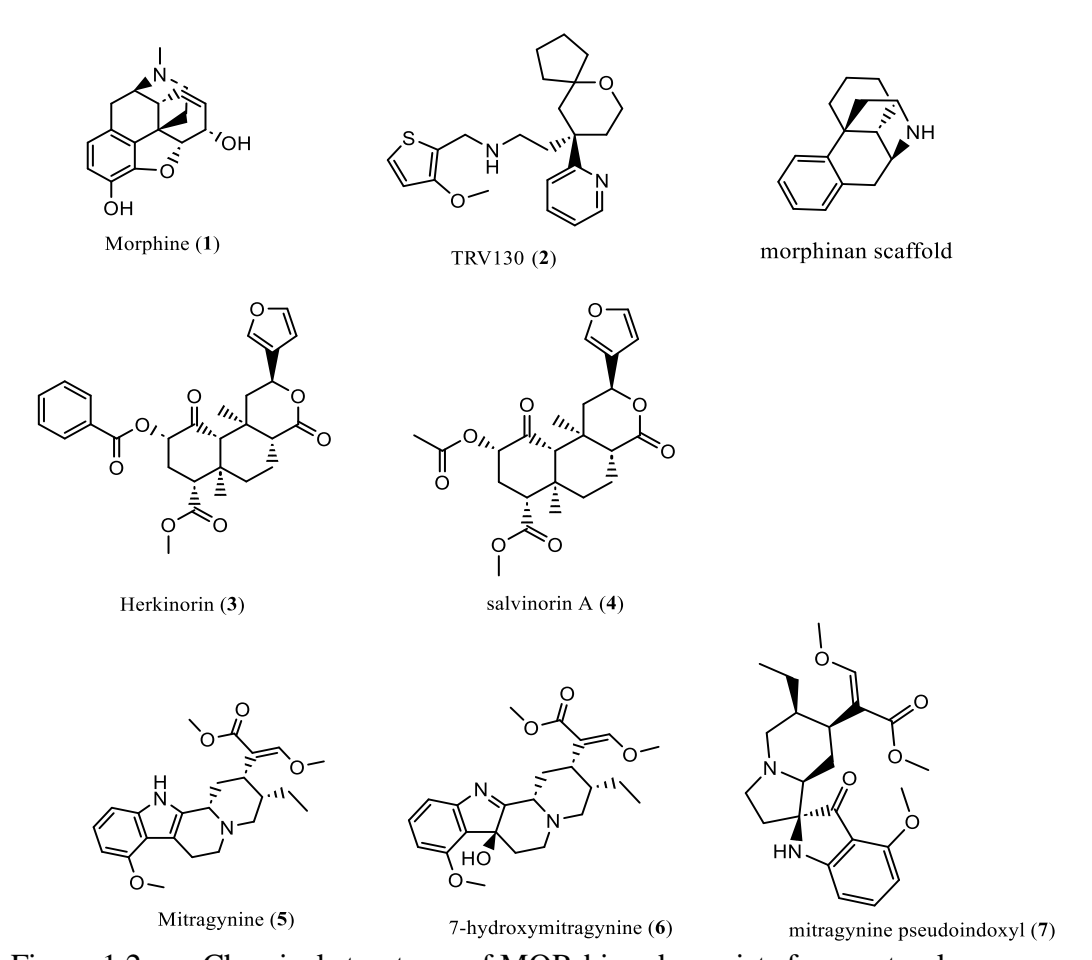


Figure 1.2 Chemical structures of MOR-biased agonists from natural resources.

(4) Using MOR structure (target) based drug design (SBDD). The SBDD methodology was applied in the discovery of the MOR-biased agonist PZM21, which was obtained through the docking of millions of compounds against MOR followed by lead optimisation (Manglik et al., 2016).

MOR agonists with a different structure other than the morphinan scaffold (Figure 1.2) might serve as a better analgesic with reduced side effects related to morphine (Váradi et al., 2016). One of the naturally occurring substances that is non-morphinan and found to possess analgesic activity is mitragynine, which is found to exert its analgesic effect by binding with opioid receptors, especially MORs (Kruegel et al., 2016, 2019). Mitragynine is an indole-based alkaloid with four-fused rings (Figure 1.3). The THβC moiety is an integrated three-fused ring which represents a simplified indole-based alkaloids of four-fused rings of mitragynine as shown in Figure 1.3.

Mitragynine

Tetrahydro-beta-carboline

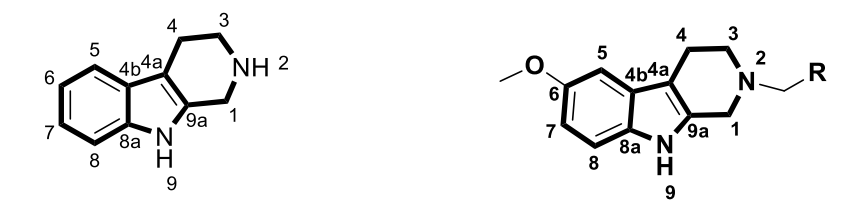


Figure 1.3 Structures of mitragynine, and tetrahydro-beta-carbolines.

6-methoxytetrahydro-beta-carboline

TH β Cs, otherwise known as tetrahydronorharmane, are natural organic betacarbolines (β Cs) derivatives. They were initially isolated from *Peganum harmala* and subsequently from other various natural resources including *Acanthostrongylophora* ingens, Annona foetida, Arenaria kansuensis, Eudistoma spp and Psilocybe mushrooms, (Blei et al., 2019; Cui et al., 2017; Ibrahim & Mohamed, 2017). Several derivatives of the THβCs have also been synthetically produced. They generally possess a structure-supporting ability of their scaffold to interact with various biological targets. As such they have been reported with a broad spectrum of pharmacological effects against several diseases and disorders including cancer, inflammation and neuropsychiatric disorders (Dai et al., 2018). They also have been demonstrated with medicinally interesting analgesic activities with reduced side effects compared with opioids (Bertamino et al., 2020; Chavan et al., 2011; Nie et al., 2020).

Problem statement

Pain remains a debilitating health condition that is affecting millions of the global population. Its clinical complications result from the unavailability of versatile drugs for effective pain management. Opioid analgesics are effectively deployed in critical clinical situations and their common types mechanistically function through the mu-opioid receptors (MORs). However, despite their efficiency in clinical pain management, all currently approved MOR analgesics including the popular morphine analogues are subjects of adverse events. These include addiction, constipation, dependence, respiratory depression and tolerance (Faouzi et al., 2020). In addition, they are mostly abused, thereby constituting public health problems. These make the development of new and effective MOR analgesic drugs with minimal side effects and fewer tendencies for drug abuse a necessary challenge. Progressively, THβC analogues are gaining arrays of scientific interest as potential neuropharmacological agents (Ayipo et al., 2021). Relevantly, they have been recently reported with

promising analgesic activities and ideal safety (Al-Azzawi, 2018). However, their potential for effective analgesic pharmacology mechanistically through the MOR remains less explored.

This study aims to develop new MOR ligands based on the TH β C scaffold and evaluate their analysis and toxicity potentials in *in vivo* zebrafish model.

1.2 Objectives

- i) To design new THβC derivatives based on fragment substitution using virtual screening, molecular docking and *in silico* ADMET predictions.
- ii) To synthesise the designed $TH\beta C$ derivatives using the Pictet-Spengler approach.
- iii) To evaluate the MOR analgesic pharmacology and toxicity effects of the synthesised THβC derivatives using *in silico* and *in vivo* zebrafish embryo

CHAPTER 2

LITERATURE REVIEW

2.1 Pain

2.1.1 Definition of pain

The International Association for the Study of Pain (IASP) defines pain as "an unpleasant sensory and emotional experience associated with actual or potential tissue damage or described in terms of such damage" (Merskey, 2007). The definition was revised as "Pain is a mutually recognisable somatic experience that reflects a person's apprehension of threat to their bodily or existential integrity" (Cohen et al., 2018). In 2020, the IASP Council proposed a revised definition of pain: "An unpleasant sensory and emotional experience associated with or resembling that associated with actual or potential tissue damage" (Raja et al., 2020). This highlighted that pain remains a broad concept.

2.1.2 Classification of pain

There are several ways to classify pain. The following section summarises the general classifications based on duration and tissue damage.

2.1.2(a) Pain classification based on duration.

2.1.2(a)(i) Acute pain

Acute pain is a healthy physiological response to a stimulus that ends with healing (Meyr & Steinberg, 2008) and usually lasts less than 3 to 6 months (Merskey, 2007).

2.1.2(a)(ii) Chronic pain

Chronic pain typically results from a disease or an injury (Mills et al., 2019). It can be defined as pain that lasts more than six months or until the injury is healed completely (Merskey, 2007).

2.1.2(b) Pain classification based on tissue damage.

2.1.2(b)(i) Nociceptive pain

Nociceptive pain can be defined as the activity in neural pathways resulting from actual tissue or potential tissue damage from exclusive stimuli (Nicholson, 2006). It is usually considered protective (Woolf, 2010). These pathways are through which the pain sensation is transmitted from painful stimuli to the brain. The counter pathways, antinociceptive pathways, are the modulation pathways of painful stimuli. They control and modulate pain due to the secretion of 5-hydroxytryptamine (5HT) and noradrenaline that leads to the activation of opioid interneurons by secretion of endogenous opioid peptides, which effectively block the propagation of pain signals through the ascending pathway (Stamford, 1995; Yam et al., 2018).

2.1.2(b)(ii) Neuropathic pain

Neuropathic pain is a pathological process caused by damage to the nervous system (Woolf, 2010). It's widely known as one of the most severe pain (Hecke et al., 2014). A combination of peripheral and central sensitisation mechanisms causes neuropathic pain. Abnormal signals are generated by injured axons and intact nociceptors that share the innervation territory of the injured nerve (Campbell & Meyer, 2006).

2.1.2(b)(iii) Nociplastic pain

A type of pain originating from modified nociception, even in the absence of definite signs of real or impending tissue harm, triggers the activation of peripheral nociceptors. Similarly, there is no proof of disease or injury in the somatosensory system causing this pain sensation as declared by IASP (*IASP Terminology*, 2018).

2.1.3 Mechanism of pain

The pain mechanism comprises four main stages: transduction, transmission, perception, and modulation through two main pain pathways progressing in opposite directions under the influence of stimuli. The ascending pathway is sometimes called the nociceptive pathway, whereas the opposite-direction pathway is termed the anti-nociceptive or descending pathway (Figure 2.1) (Martyn et al., 2019).

Painful stimuli are controlled and modulated through the pathways in which painful stimuli are converted into chemical tissue events from the place of injury to the somatosensory cortex, part of the cerebral cortex where the information is integrated, and the perception of pain is perceived.

Opioid receptors are expressed in pain-modulating descending pathways, which include the medulla locus coeruleus, and periaqueductal gray area (Al-Hasani & Bruchas, 2011). White blood cells, known as leukocytes, are released at the site of injury. These cells secrete naturally occurring opioid peptides, which then engage with the opioid receptors that have been up-regulated along nerve terminals due to the injury. As a result of this interaction, pain is diminished. This intricate process involves the body's innate response to injury, where the release of endogenous opioids serves as a mechanism to alleviate the discomfort associated with the damage. The heightened

presence of opioid receptors near nerve endings underscores the body's adaptive measures to modulate pain perception in response to injury. (Stein, 2016).

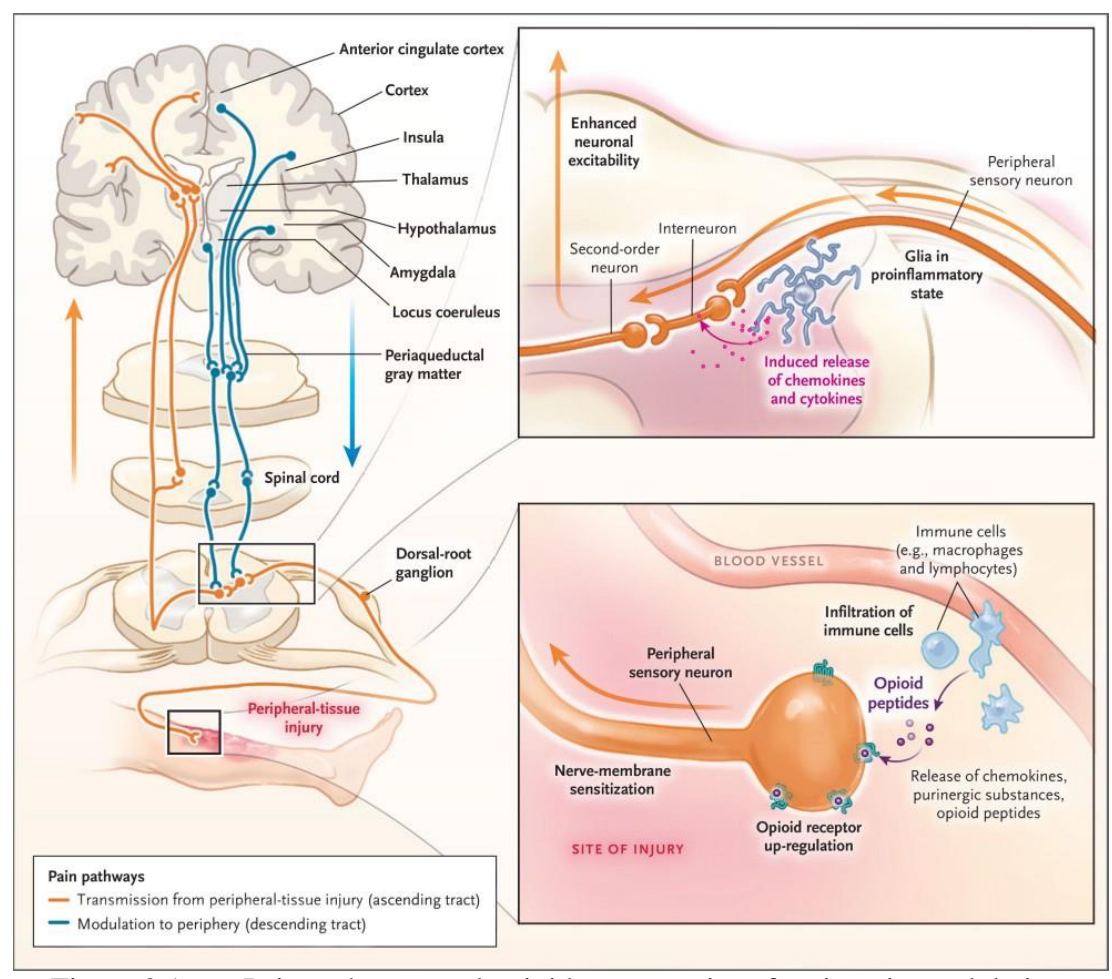


Figure 2.1 Pain pathways and opioid receptors interfere in pain modulation, adopted from Martyn et al., 2019.

2.2 G Protein-Coupled Receptors (GPCRs) Structure and Function

G protein-coupled receptors (GPCRs) are a superfamily of membrane proteins, also called seven transmembrane receptors (7TMRs), found in all tissue types, including the central nervous system (Rosenbaum et al., 2009). The GPCRs are encoded in about 3% of the human genome (Fredriksson et al., 2003). In 2000, Palczewski and coworkers determined the first three-dimensional (3D) structure of a GPCR rhodopsin with 2.8 angstroms (Å) resolution in its inactive, dark-adapted state (PDB ID: 1F88)

(Palczewski et al., 2000). After seven years, the crystal structures for the β- adrenergic receptor family members were identified. Due to the improvements in crystallisation techniques as well as its instrumentations (i.e., high-resolution X-ray, Nuclear Magnetic Resonance (NMR), and cryogenic electron microscopy (cryo-EM)), the number of GPCR crystal structures is believed to tremendously increase to about 793 by 2022 (http://gpcrdb.org/structure/statistics) (Kooistra et al., 2021). The GPCRs consist of seven transmembrane helices (TM1-TM7) connected by three intracellular loops (ICLs) ended with helix 8 (H8), and three extracellular loops (ICLs) ended with N-terminal pointed out (Figure 2.2).

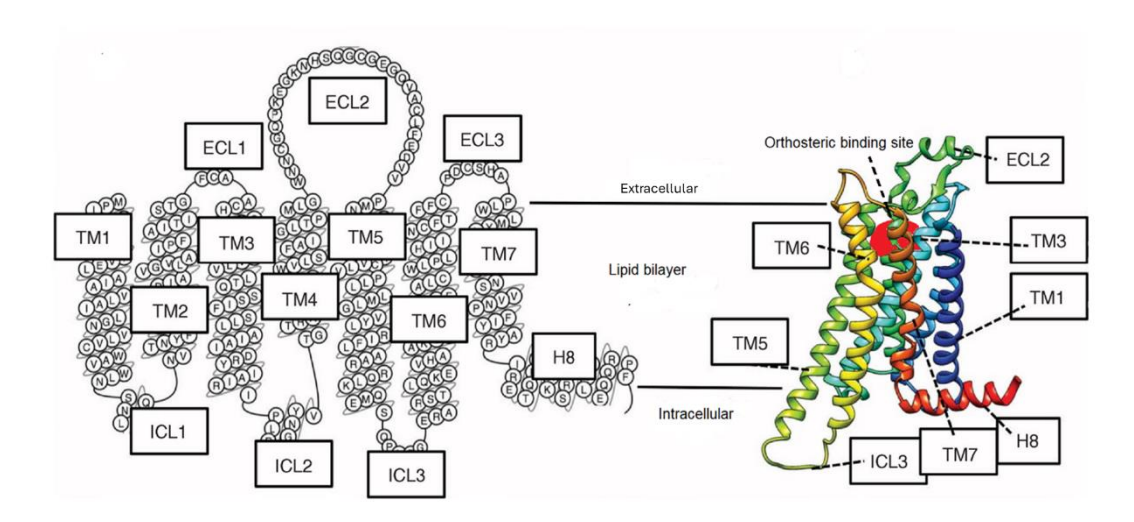


Figure 2.2 Structure of a G protein-coupled receptor (GPCR). (a) GPCR snake presentation (adopted from www.gpcrdb.org) showing the main structural features; transmembrane helices (TMs), C-terminal helix 8 (H8), extracellular loops (ECLs), and intracellular loops (ICLs) (b) Tertiary ribbon representation of the GPCR structural features including orthosteric binding site.

The GPCRs recognise and respond to a variety of stimuli (exogenous and endogenous signals from ions to peptides) (Wu et al., 2017), which makes them crucial in regulating multi-physiological and biological processes required to coordinate cellular activities, including cardiovascular, neurological, and endocrinal functions (Galligan J.J., 2016; Nagarajan et al., 2014). Due to their importance and functions, the GPCRs are considered major therapeutic drug targets. However, GPCRs contain two

druggable binding sites (orthosteric and allosteric). Endogenous ligand usually binds to orthosteric sites within the cavity exposed to the extracellular side of the TMs (Figure 2.2). In contrast, modulators bind to allosteric sites, making them both accessible to different ligands, including drugs (Wootten et al., 2013). The extracellular ligands stabilise particular receptor conformational ensembles interacting with suitable intracellular mediators by defined affinities (Hauser et al., 2021). Thus each ligand has a specific affinity determined by its dissociation constant from the extracellular part of the receptor and specific efficacy determined by the type and extent of receptor-induced interaction with intracellular mediators (Mahmod Al-Qattan & Mordi, 2019).

2.3 Mu Opioid Receptor (MOR)

Opioid Receptors (OR), members of the GPCR, are expressed and distributed along the central nervous system (Sora et al., 1997), peripheral nervous system (Ozawa et al., 2015), the gastrointestinal tract (Galligan, 2016; Sobczak et al., 2014). The mu, delta, and kappa opioid receptor subtypes have been identified to be closely associated with pain perception and modulation (Higginbotham et al., 2022). The MOR mediates the most potent antinociceptive effects, the most powerful analgesic, and the addictive properties of opiate alkaloids. Therefore MOR are considered a primary target in developing new analgesics (Law et al., 2013; Pradhan et al., 2012). Currently, MOR crystal structures are available with a bound agonist of BU72 (PDB ID: 5C1M), the bound antagonist of BF0 (PDB ID: 4DKL), and bound intracellular Gi protein (PDB ID: 6DDE) (Huang et al., 2015; Manglik et al., 2012; Koehl et al., 2018).

Ligands binding to MOR may induce intracellular interaction of Gi protein, referred to as agonistic activity, or block the interaction of other agonists, referred to as antagonists. The activation of GPCR by extracellular ligands induces either transient or

long-lasting intracellular signals by activating either G proteins or beta-arrestins (van Gastel et al., 2018). Signalling through G proteins leads to pain relief while signalling through beta-arrestin induces respiratory depression (Law et al., 2013).

Activation of the MOR results in signalling through the heterotrimeric G protein Gi, resulting in analgesia, sedation, euphoria, and physical dependence (Chan et al., 2017). The classification of agonists is based on their pharmacological response, and it primarily distinguishes between two main categories: full agonists and partial agonists. These distinctions arise from the way these compounds interact with MOR. Full agonists exert their effects by binding to the orthosteric site of the receptor. Once bound, they effectively stabilise the active conformation of the MOR, inducing a comprehensive and maximal biological response. This means that when a full agonist engages with the receptor, it triggers the receptor to its maximum potential, resulting in a robust and complete physiological effect. This binding and stabilisation process elicits a response equivalent to the endogenous ligand's activation of the receptor. On the other hand, partial agonists also bind to the same orthosteric site on the receptor, but their impact on the biological response is distinct. Despite binding to the receptor, partial agonists do not induce the receptor to reach its maximum potential response, even when present at higher concentrations. Instead, they elicit a partial biological response compared to full agonists. This characteristic is a crucial aspect of their pharmacological profile, as partial agonists may act as modulators, exerting a more nuanced influence on receptor activity (Manglik et al., 2015; Nygaard et al., 2013).

MOR agonists, including morphine, are clinically used to treat moderate to severe chronic pain (Trescot et al., 2008). In contrast, the MOR antagonists competitively prevent resting MOR activation, while common antagonists, such as

naloxone and naltrexone, also bind to and block ligand-free MOR, acting as potent inverse agonists and serving as pain modulators (Sum et al., 2019). Selective activation of the Gi/o pathway over the beta-arrestin pathway by biased signalling is recommended for analgesics deprived of respiratory and addictive side effects.

Opioid chemistry has been driven by thebaine-derived alkaloids isolated from poppy, such as morphine (Carlin et al., 2020). There is an increase in the number of opioids containing natural products with structures other than the morphinan scaffold and structures that are not closely related to morphine, such as mitragynine (Váradi et al., 2016).

2.4 Structure-Based Drug Design (SBDD)

In drug discovery and development, there is a continuous need to search for procedures that save money and time and reduce failure. This has led to the development of artificial intelligence (computational techniques) to serve as a complement to conventional drug discovery techniques. Therapeutic pharmacology aims to develop highly selective drugs with no side effects. Phenotypic screening-based drug design was the major method used in drug discoveries where leading compounds are developed based on disease models (Eder et al., 2014). Until target-based screening came into existence first in 1976 (Beddell et al., 1976), target-based drug design was termed Computer-Aided Drug Design (CADD) (Sotriffer & Klebe, 2002). In CADD, millions of compounds can be screened against target proteins effectively and efficiently. As a consequence of the development in methods concerning protein isolation, purification and crystallisation, 3-Dimensional (3D) structures of target proteins were determined with the aid of several techniques, including x-ray crystallography, Nuclear Magnetic Resonance Spectroscopy (NMR) and Cryo-cooling techniques(Verlinde & Hol, 1994;

Batool et al., 2019). Structure-Based Drug Design (SBDD) has been established as a new category in drug discovery and development (Wang et al., 2018). The SBDD is considered the most efficient tool in drug discovery and development (Verlinde & Hol, 1994; Batool et al., 2019; Ballante et al., 2021), as well as convenient in terms of speed and cost.

2.4.1 Structure-Based Drug Design Workflow

The SBDD process starts first with identifying the target protein, followed by screening libraries of compounds against the target using docking. Following hit selection and evaluations, the most active compounds can be optimised (hit-to-lead) to improve their pharmacodynamical profile, such as efficacy and affinity. The main steps in the SBDD technique include; 3D protein structure preparation, binding site identification, ligands database generation, docking and scoring (Wang et al., 2018), testing of the hit compounds, and identifying the lead compound (Batool et al., 2019). The overall workflow of SBDD is shown in Figure 2.3.

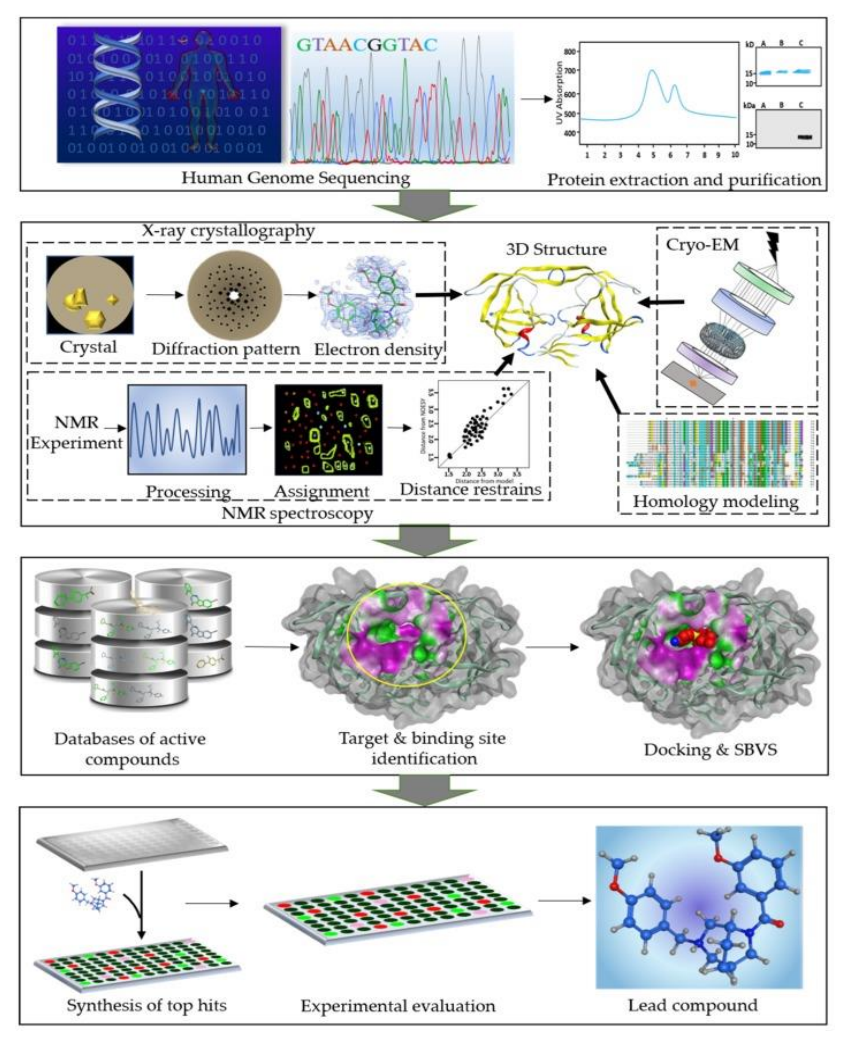


Figure 2.3 A workflow diagram of the structure-based drug design (SBDD) process. Obtained from Batool et al., 2019.

2.4.2 SBDD and opioid receptors ligands

Opioid receptors (OR) are the G protein-coupled receptor (GPCR) superfamily members. The OR is composed of three main receptors: Mu Opioid Receptor (MOR), Kappa Opioid Receptor (KOR), and Delta Opioid Receptor (DOR). The most recently found member is the NOP receptor (nociceptin/orphanin' opioid peptide receptor) (Manglik, 2020; Toll et al., 2016). The ORs are found mainly in the central nervous system (CNS) and peripheral nervous system, making them therapeutic targets in pain modulations (Manglik, 2020; Pasternak & Pan, 2013). It has been found that the great emphasis on pain modulation is referred to as MOR activation. However, the other ORs

have different degrees of pain modulation, considering the signalling pathways following their binding with the drugs (Valentino & Volkow, 2018).

Herein, this study focused more on MOR as it was used as a target receptor. The first crystal structure of MOR to be determined was the in-active MOR binding to morphinan antagonist (PDB ID: 4DKL) by Manglik and coworkers (Manglik et al., 2012) with 2.80 Å resolution using X-ray diffraction. In 2015, Huang and coworkers were able to crystalise active MOR binding to Agonist BU72 (PDB ID: 5C1M) with 2.1 Å resolution using x-ray diffraction. In 2018, the Koehl research group obtained active MOR bound to the agonist peptide DAMGO and nucleotide-free G_i (PDB ID: 6DDE; 6DDF) (Koehl et al., 2018) with 3.5Å resolution using the Cryo-EM technique. Herein, the latest (i.e., 6DDE) was used as the target for SBDD.

MOR activation via the Gi protein pathway is associated with desired analgesic effects. However, MOR can also signal through arrestin, contributing to the undesired effects of opioid analgesics such as tolerance, respiratory suppression, and constipation.(Bohn et al., 2000; Raehal et al., 2005). The efforts in drug discovery and development are to discover analgesics that will provide more effective relief of pain with minimum side effects reported for opioids, such as respiratory depression, addiction, constipation, nausea, and vomiting (Kalso et al., 2004). The use of SBDD to discover opioid receptor ligands became state-of-the-art (Lee et al., 2018). An example of using SBDD to discover MOR ligand was a compound retrieved by Manglik et al., (2016) after screening more than 3 million compounds against MOR followed by hitto-lead optimisation, which led to the discovery of PZM21(EC $_{50} = 4.6$ nM, Ki =1.1 nM) Gi-biased MOR agonist. This study aimed to perform a structure-based design of MOR ligands using a library of Tetrahydro-beta Carboline (TH β C) analogues.

2.5 Tetrahydro-beta-carbolines (THβC's)

This section summarises the occurrence, synthesis, and biological activity of $TH\beta C$'s, with a focus on its role in pain modulations.

2.5.1 Tetrahydro-beta-carbolines (THβC's) occurrence

Organic compounds of natural origins are still the key to drug discovery and development (Harvey et al., 2015; Atanasov et al., 2015; Newman & Cragg, 2016). Beta carbolines (β Cs), such as harmane, norharmane and harmine, are groups of indole alkaloids widespread in nature, such as plants, food, marine organisms, fungi, animal tissues, and human fluids (Dai et al., 2018). The β Cs were originally isolated from *Peganum harmala* (Zygophillaceae, Syrian Rue), which was used as a traditional herbal drug in the Middle East and North Africa (Cao et al., 2007). β Cs possess important pharmacological activities, including; anxiolytic, hypnotic, anticonvulsant, antitumor, antiviral, antiparasitic, or antimicrobial (Szabó et al., 2021). It is also known for its tricyclic pyrido[3,4-*b*]indole system with rings A, B and C (Figure 2.4) with different degrees of saturation at C-ring; fully saturated β -Carbolines (β Cs), partially unsaturated 3,4-dihydro- β -carbolines (DH β Cs) and fully unsaturated 1,2,3,4-tetrahydro- β -carbolines (TH β Cs). Here more focus will be given to the TH β C as it's the main purpose of this work.

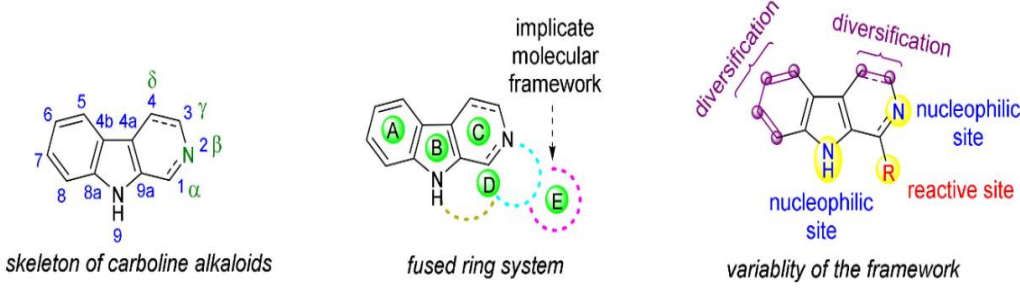


Figure 2.4 General structure of carboline alkaloids with the active sites for substitution. Adopted from Szabo et al., 2021.

Tetrahydro-β-carbolines (THβCs), or tetrahydronorharmane, are natural organic beta-carbolines (βCs) derivatives. They are a group of indole alkaloids with medicinally promising activities, including; anti-inflammatory (Demerson et al., 1975; Wrobleski et al., 2003), phosphodiesterase type 5-inhibitory (Daugan et al., 2003), antimalarial (Davis et al., 2010), antitumor (Skouta et al., 2012), antiviral, and analgesic activities (Chavan et al., 2011; Jinyu Li et al., 2019; Nie et al., 2020; S. Wang et al., 2016).

2.5.2 Tetrahydro-beta-carbolines (THβC's) methods of synthesis

Ame Pictet and Theodor Spengler first introduced the most common protocol in TH β C moiety synthesis in 1911, where 1,2,3,4-tetrahydroisoquinoline (THIQ) was produced by heating a mixture of β -phenylethylamine and formaldehyde dimethyl acetal in the presence of hydrochloric acid (Pictet & Spengler, 1911). The first synthetic TH β C (1-Methyl-1,2,3,4-tetrahydro- β -carboline) skeleton was reported in 1928 by Tatsui et al. (Tatsui, 1928) when tryptamine was used as the amine structure instead of β -phenylethylamine with acetaldehyde in the presence of sulfuric acid (Scheme 2.1).

a)
$$NH_{2}$$

$$NH_{3}$$

$$NH_{2}$$

$$NH_{2}$$

$$NH_{3}$$

$$NH_{4}$$

$$NH_{4}$$

$$NH_{4}$$

$$NH_{4}$$

$$NH_{5}$$

$$NH_{2}$$

$$NH_{2}$$

$$NH_{2}$$

$$NH_{3}$$

$$NH_{4}$$

$$NH_{4}$$

$$NH_{4}$$

$$NH_{5}$$

$$NH_{5}$$

$$NH_{2}$$

$$NH_{2}$$

$$NH_{3}$$

$$NH_{4}$$

$$NH_{4}$$

$$NH_{5}$$

Scheme 2.1 Synthesis of THIQ **2** and THβC **4** via Pictet-Spengler reaction. Obtained from Cox & Cook, 1995.

The Pictet-Spengler reaction was later optimised by Cox et al. (Cox & Cook, 1995) and validated with different amine components. Later on, a variety of catalysts were introduced, such as trifluoroacetic acid (TFA) (Miller et al., 2010), acetic acid

(AcOH) (Abdelwaly et al., 2017), p-toluenesulfonic acid (PTSA or p-TsOH) (Ye et al., 2017). Another method, but rarely used, to synthesise TH β C due to its multi-step reaction with low yields is Bischler-Napieralski cyclisation (Bischler & Napieralski, 1893). In this method, tryptamine **5** is cyclised with a dehydration reagent (such as POCl₃) to produce DH β C **6**, followed by a further reduction to form the corresponding TH β C **7**, the reaction is presented in Scheme 2.2, (Laine et al., 2014).

Scheme 2.2 Bischler-Napieralski reaction/cyclisation reaction scheme. Obtained from Laine et al., 2014.

Although the conventional protocols of THβC synthesis are validated as a straightforward way to obtain desired THβC analogues, this strategy has been modified to meet the demands related to efficiency, stereochemistry, and selectivity. These modifications include transition metal catalysis, biocatalytic methods, and microwave/ultrasound-assisted methods were also reported.

Bandini et al. reported the synthesis of TH β C analogues in 2006 using Pd-catalysed intramolecular allylic alkylation to replace conventional Freidel-Craft alkylation of indoles. The reaction was carried out under basic conditions (lithium carbonate (Li₂CO₃)) in dichloromethane (DCM) in the presence of [PdCl(π -allyl)]₂ catalysts at room temperature. The 4-Vinyl-TH β Cs **10a-h** were obtained in high yields (45 – 98%) by inter- and intramolecular allylic alkylation of compounds **9a-h** in a regioselective manner (Table 2.1) (Bandini et al., 2006).

Table 2.1 Proving the generality of the intramolecular allylic alkylation for the synthesis of 4-vinyl-TH β Cs (Bandini et al., 2006).

In 2012, Ascic et al. introduced a new method in the THβC synthesis that relies on metal-catalysed isomerisation of N-allyl tryptamines (Ascic et al., 2012) in the presence of various types of Rh-, Pd-and Ru-based catalysts without the need for an acidic or basic medium. In the Pectet-Spengler mechanism, N-allyl tryptamine 11 condensed with an aldehyde in an acidic medium to form the iminium ion intermediate 12, after which cyclisation occurs to form the THβC 13 (Scheme 2.3a). While in the metal-catalysed mechanism, allyl halide was condensed with N-allyl tryptamine 11 instead of aldehyde, and the generation of the THβC 13 cyclisation process occurred under the influence of the metal catalyst. Wilkinson's catalyst (Rh(PPh₃)₃Cl) and Ru alkylidene catalyst Ru(PCy₃)(MPI)(PM)Cl₂ were the most efficient. The THβCs were obtained in 26–94% yield with no diastereoselectivity of the applied catalysts (Scheme 2.3b).